Electron and orbital correlations in $Ca_{2-x}Sr_xRuO_4$ probed by optical spectroscopy

J. S. Lee,[1] Y. S. Lee,[2] T. W. Noh,[1,†] S.-J. Oh,[2] Jaejun Yu,[2] S. Nakatsuji,[3,‡] H. Fukazawa,[3] and Y. Maeno[3]

[1]*School of Physics and Research Center for Oxide Electronics,*
Seoul National University, Seoul 151-747, Korea
[2] *School of Physics and Center for Strongly Correlated*
Materials Research, Seoul National University, Seoul 151-747, Korea
[3]*Department of Physics, Kyoto University, Kyoto 606-8502, Japan*

(July 17, 2002)

Abstract

The doping and temperature dependent optical conductivity spectra of the quasi-two-dimensional $Ca_{2-x}Sr_xRuO_4$ ($0.0 \leq x \leq 2.0$) system were investigated. In the Mott insulating state, two electron correlation-induced peaks were observed around 1.0 and 1.9 eV, which could be understood in terms of the 3-orbital Hubbard model. The low frequency peak showed a shift toward higher frequency as temperature was lowered, which indicated that electron-phonon interactions play an important role in the orbital arrangements. From the systematic analysis, it was suggested that the antiferro-orbital and the ferro-orbital ordering states could coexist.

PACS number: 78.20.Ci, 71.27.+a, 71.30.+h, 78.30.-j

Typeset using REVTeX

The discovery of unconventional superconductivity in Sr_2RuO_4 has stimulated great interest in layered perovskite $Ca_{2-x}Sr_xRuO_4$ ($0.0 \leq x \leq 2.0$) (CSRO) [1,2]. The normal state of Sr_2RuO_4 can be described as a quasi-two dimensional Fermi-liquid [3]; however, the isovalent Ca substitution for Sr gives rise to a Mott insulator Ca_2RuO_4 [4]. As x decreases, the RuO_6 octahedra rotate and become flattened [5]. These structural distortions decrease the Ru $4d$ bandwidth W, which leads to a Mott gap. Therefore, CSRO can be used as a prototype material system to investigate the evolution of electronic structures from a band metal to a Mott insulator.

The role of the orbital degrees of freedom in Ca_2RuO_4 has provided us with a challenge of scientific interest. The Ru ion has a formal valency of 4+ with four t_{2g} electrons. At an early stage, it was proposed that the d_{xy} orbitals should be fully occupied and that a Mott gap becomes open between the half-filled $d_{yz/zx}$ states [6]. However, recent x-ray absorption spectroscopy (XAS) data revealed that both d_{xy} and $d_{yz/zx}$ orbitals remain partially filled down to low temperature (T) [7]. Then, it would be difficult to understand how the Mott insulator can be formed with partially filled d_{xy}, d_{yz}, and d_{zx} orbitals. More recently, using the 3-orbital Hubbard model, Hotta and Dagotto suggested that the unusual orbital occupancy could be explained by an antiferro-orbital (AFO) ordering in the antiferromagnetic (AFM) state [8].

Optical spectroscopy has been used as a powerful method to investigate electronic structures of numerous strongly correlated materials [9]. However, most of the observed correlation-induced features have been interpreted in terms of the single-band Hubbard model without considering the orbital degeneracy. Recently, optical spectroscopy was applied to probe the role of orbital ordering in polaron absorption of perovskite manganites; even with similar orbital occupancy, optical absorption can vary significantly depending on the orbital correlation between nearest neighbors [10]. Therefore, optical spectroscopy can provide us with a way to investigate the role of orbitals in the intriguing electronic states of CSRO.

In this Letter, we investigate the doping- and T-dependent optical conductivity spectra $\sigma(\omega)$ of CSRO. In the insulating state, $\sigma(\omega)$ show two correlation-induced excitations around 1.0 and 1.9 eV. These features are explained in terms of the 3-orbital Hubbard model, which considers the t_{2g} orbital multiplicity. In the Mott insulating state, the AFO correlation is prevalent, but the ferro-orbital (FO) correlation seems to coexist with decrease of T. It is also found that the electron-phonon interaction plays an important role in the T-dependent evolution of the orbital arrangements.

High-quality CSRO single crystals were grown by the floating zone method. Details of the crystal growth and characterization were described elsewhere [11]. Near normal incident reflectivity spectra, $R(\omega)$, of the ab-plane were measured between 5 meV and 30 eV. Using a liquid He-cooled cryostat, T-dependent $R(\omega)$ were obtained below 5.0 eV. Using Kramers-Kronig analysis, $\sigma(\omega)$ were obtained [12].

Figure 1 shows $\sigma(\omega)$ of CSRO at room T. For Sr_2RuO_4, $\sigma(\omega)$ has a strong Drude-like peak, indicating its metallic state. As x decreases, the Drude-like peak becomes gradually suppressed. For Ca_2RuO_4, $\sigma(\omega)$ shows an insulating response with an optical gap. These spectral changes are consistent with the metal-insulator (MI) transition observed in dc resistivity ρ_{dc} [2]. The strong peak around 3.0 eV can be assigned to the p-d transition from the O $2p$ to the unoccupied Ru t_{2g} states, just like in earlier works on numerous ruthen-

ates [13–15]. Therefore, the spectral features below 2.5 eV should originate from transitions between the Ru $4d$ bands.

The spectral weight changes in Fig. 1 can be understood according to the Mott-Hubbard picture. As x decreases, the structural distortions become larger [5], which makes W of the Ru $4d$ orbitals narrower. As U/W increases (U is the electron correlation energy.), the Hubbard bands develop with reduction of the quasi-particle peak centered at the Fermi energy [16]. Figure 1 shows that an additional peak develops around 2.0 eV as x decreases. To identify this peak more easily, each spectrum is subtracted by $\sigma(\omega)$ of x=2.0 and plotted as $\Delta\sigma(\omega)$ in the inset of Fig. 1. The spectral weight redistributions between the coherent and the incoherent excitations can be understood in the W-controlled Mott-Hubbard picture. Then, the 2.0 eV excitation should be assigned as the so-called 'U-peak', i.e., the optical transition from the lower Hubbard band to the upper Hubbard band.

The increase of U/W should lead to an AFM Mott insulator. For its $\sigma(\omega)$, only one correlation-induced peak was usually reported [16]. However, $\sigma(\omega)$ of the x=0.0 sample exhibits two separate peaks around 1.0 and 1.9 eV. Earlier, Puchkov et $al.$ reported $\sigma(\omega)$ of Ca_2RuO_4 up to 1.3 eV and assigned the low energy peak to the U peak [14]. The high energy peak corresponds to the 2.0 eV excitation in the metallic CSRO. If both peaks come from the electron correlation effects, the single-band Hubbard model cannot explain the appearance of these two peaks. Moreover, the simple picture cannot explain the recent XAS studies, which reported a dramatic redistribution of orbital occupancies [7].

To obtain further insights, we investigated $\sigma(\omega)$ of the x=0.06 sample, which undergoes an MI transition below room T [17]. The inset of Fig. 2(a) shows that ρ_{dc} experiences an abrupt jump at $T_{MI} \sim 220$ K with decreasing T, which is closely related to the first-order structural transition [5]. Figure 2(a) shows the T-dependent $\sigma(\omega)$, where the sharp spikes below 0.1 eV are due to transverse optic phonons. Consistent with ρ_{dc}, $\sigma(\omega)$ also show the first-order nature of the MI transition; below T_{MI}, the strong coherent peak suddenly disappears and an optical gap appears with the 1.0 eV peak (Peak α), accompanied by a slight enhancement of the 1.9 eV peak (Peak β). The new Peak α does exist in the insulating region of the x=0.06 sample as well as in the room-T $\sigma(\omega)$ of the x=0.0 sample. [Note that T_{MI} for the x=0.0 sample is around 357 K [18].] Thus, the two-peak structure can be regarded as an ubiquitous feature of the Mott insulating state in CSRO.

Note that there exist systematic spectral changes below 2.5 eV even in the insulating state. In order to illustrate these changes clearly, we subtracted the contributions of the phonons and the p-d transitions, indicated as a dot-dot-dashed line in Fig. 2(a), from each spectrum to obtain the contribution of the transitions between $4d$ states, $\sigma_{4d}(\omega)$. Figure 2(b) shows the two-peak structure of $\sigma_{4d}(\omega)$. As T decreases, the spectral weight of Peak α (S_α) decreases, but that of Peak β (S_β) increases. The sum of the spectral weights up to 3.0 eV remains the same, satisfying the optical sum rule. It should be noted that only Peak α shows the T-dependent peak shift.

To explain these spectral changes, we consider the 3 t_{2g}-orbital Hubbard model. When the orbital multiplicity is taken into account, the Hund's rule exchange energy J between t_{2g} electrons should play an important role. The interactions among electrons on the same site can be described by U Coulomb repulsion energy (CRE) between two electrons in the same orbital, U' CRE between two electrons in different orbitals with opposite spins, and U'' CRE between electrons in different orbitals with the same spin. [When the rotational

symmetry in the orbital space is considered, $U' = U - 2J$, and $U'' = U - 3J$ [19].] As shown in Fig. 3, the energy cost of the d-d transition (i.e., $d^4 + d^4 \longrightarrow d^3 + d^5$) depends on the spin and the orbital configurations of the nearest neighboring Ru ions. For the time being, let us assume that all of the t_{2g} states are degenerate. Then, we should consider four kinds of spin/orbital configurations. Figure 3(a), (b), (c), and (d) show possible d-d transitions in FM (ferromagnetic)/FO, FM/AFO, AFM/FO, and AFM/AFO configurations, respectively. [Here, FO (or AFO) implies that the same (or different) t_{2g} orbitals are occupied in the two sites.] With the above mentioned CRE's, the corresponding energy costs of the d-d transitions are estimated. As shown in Fig. 3, the FM/FO configuration does not allow any d-d transition. And, the FM/AFO and the AFM/FO configurations allow only one transition. On the other hand, the AFM/AFO configuration allows two transitions with energy costs of $U - J$ and $U + J$ [20].

How can we understand the two-peak structure? Note that the *Néel* temperature T_N of the x=0.06 sample is around 150 K [21]. Near and below T_N, the nearest neighbor spin correlation is mostly AFM, so most excitations come from the AFM/AFO and the AFM/FO configurations. Then, Peaks α and β can be assigned as excitations of $U - J$ and $U + J$, respectively. From the energy difference between two excitations, the value of $2J$ can be estimated to be about 1 eV. It is in good agreement with the earlier reports [22], thus demonstrating the validity of our peak assignments.

The T-dependent spectral weight changes in Fig. 2(b) can be understood as a result of changes of the AFO and the FO correlations. Using the Lorentzian fittings, we estimate S_α and S_β [23]. Since the value of S_α is similar to that of S_β at most temperatures, the contribution of the AFO correlation seems to be more prevalent than that of the FO correlation. Figure 4 shows the T-dependent spectral weight changes of S_α and S_β. As T decreases, S_α decreases, but S_β increases. These T-dependences suggest that the FO correlation increases with decreasing T. Then, it can be said that there is a competition between AFO and FO configurations at least in the ground state of the x=0.06 sample.

Another interesting feature is that Peak α shifts to higher frequencies by about 0.24 eV with decreasing T, but Peak β does not shift significantly. Note that U and J values for most solids have little T-dependences. To explain this intriguing behavior, we pay attention to the electron-phonon (*el-ph*) coupling. As T decreases, it was known that the RuO$_6$ octahedra rotate and become flattened [5]. The inset of Fig. 2(b) shows the phonon spectra of the in-plane Ru-O stretching mode [24]. As T decreases, the phonon frequency ω_{TO} decreases rather significantly, which suggests an increase of the in-plane Ru-O bond length (i.e., the flattening of the octahedron). In addition, the strong *el-ph* coupling makes the phonon lineshape asymmetric, in agreement with Raman measurements [25]. Figure 4 also shows that the changes of ω_{TO} and $\Delta S_\alpha(T)$ could be related.

Now, let us consider the *el-ph* coupling energy E_{ph}. Note that the Ru ions with 4 t_{2g} electrons cannot have degenerate t_{2g} levels. Due to the strong Jahn-Teller-like distortion, the energy levels of the doubly and the singly occupied orbitals will change by -2E_{ph} and E_{ph}, respectively [8]. For example, let us consider the orbital polarized state, shown in Fig. 3(e), which is composed of two sites with doubly occupied d_{xy} and d_{yz} orbitals. Its schematic energy level with the Jahn-Teller-like distortion is shown in Fig. 3(f). Compared to the degenerate case, the orbital polarized state with the AFM/AFO configuration will have an additional energy cost of $3E_{ph}$ in the $U - J$ excitation, so the position of Peak α

should be located at $U - J + 3E_{ph}$. However, the $U + J$ excitation contributing to Peak β remains independent of the lattice distortion. With $E_{ph} \sim \omega_{TO} \sim 600$ cm^{-1} ($\simeq 0.074$ eV), the shift of Peak α is estimated to be about 0.22 eV, in agreement with our experiment. The continuous shift of the $U - J$ excitation can be explained by the fact that short range orbital orderings, which accompanies the lattice distortion in Fig. 3(e), grows progressively. Near T_N, corresponding long range orbital orderings become stabilized and most of the spectral weights will move to $U - J + 3E_{ph}$. Our work demonstrates that the *el-ph* coupling should be strong in CSRO and play an important role in the evolution of the orbital degree of freedom. The shift of ω_{TO}, due to the stong *el-ph* coupling, should be closely related with the orthorhomic distortion. This distortion will suppress the AFO ordering [6] and can explain the close relation between ω_{TO} and $\Delta S_\alpha(T)$, observed in Fig. 4.

To explain the electronic structure of the Ca_2RuO_4 Mott insulating state, Anisimov *et al.* proposed an FO ordered state of the d_{xy} orbitals [6]. This intriguing state can explain a Mott gap in the half-filled $d_{yz/zx}$ state and an orthorhombic lattice distortion. Recently, Hotta and Dagotto proposed another interesting AFO ordered state, stabilized by a combination of the correlation and the *el-ph* coupling effects [8]. In the AFO ordered state (shown in Fig. 1(e) of Ref. [8]), the two-dimensional network composed of d_{xy} orbitals is occupied in a bipartite manner by half of the excess t_{2g} electrons. The other excess electrons occupy d_{yz} and d_{zx} orbitals. The related lattice distortions should occur in pairs, resulting in a cooperative distortion in the total in-plane lattice. Our observation of the prevalence of the AFO correlation and the energy shift of the $U - J$ excitation seem to be consistent with the latter picture. However, the increase of the FO at lower T cannot be simply explained.

One possible scenario is the phase coexistence of the FO and the AFO ordered states in the insulating CSRO. In the two-dimensional square network, the AFO ordered state will be preferred, since it provides the kinetic energy gain by allowing hoppings between the nearest neighbors [8]. On the other hand, with the orthorhombic lattice distortion, the FO ordered state will be preferred [6]. If the energy difference between two states is small, the FO and the AFO ordered Mott insulating states can coexist. Then, the insulating CSRO will be in an interesting state composed of two kinds of Mott insulators. Further works are required to verify this intriguing possibility.

In summary, we investigated the doping- and temperature-dependent optical conductivity spectra of $Ca_{2-x}Sr_xRuO_4$. Based on the 3-orbital Hubbard model, we could explain the two correlation-induced excitations. Moreover, from their spectral weight changes, we found that the electron-phonon coupling plays an important role in the dynamics of the spin/orbital correlations. We also proposed the possible phase coexistence of orbital ordered states in the insulating samples.

REFERENCES

[†]   corresponding author, *e*-mail: twnoh@phya.snu.ac.kr

[‡]   present address: NHMFL, Tallahassee, Florida 32310

[1] Y. Maeno, H. Hashimoto, K. Yoshida, S. Nishizaki, T. Fujita, J. G. Bednorz, and F. Lichtenberg, Nature (London) **372**, 532 (1994).

[2] S. Nakatsuji and Y. Maeno, Phys. Rev. Lett. **84**, 2666 (2000).

[3] A. P. Mackenzie, S. R. Julian, A. J. Diver, G. J. McMullan, M. P. Ray, G. G. Lonzarich, Y. Maeno, S. Nishizaki, and T. Fujita, Phys. Rev. Lett. **76**, 3786 (1996).

[4] S. Nakatsuji, S. Ikeda, and Y. Maeno, J. Phys. Soc. Jpn. **66**, 1868 (1997).

[5] O. Friedt, M. Braden, G. Andre, P. Adelmann, S. Nakatsuji, and Y. Maeno, Phys. Rev. B **63**, 174432 (2001).

[6] V. I. Anisimov, I. A. Nekrasov, E. E. Kondakov, T. M. Rice, and M. Sigrist, Eur. Phys. J. B **25**, 191 (2002).

[7] T. Mizokawa, L. H. Tjeng, G. A. Sawatzky, G. Ghiringhelli, O. Tjernberg, N. B. Brookes, H. Fukazawa, S. Nakatsuji, and Y. Maeno, Phys. Rev. Lett. **87**, 077202 (2001).

[8] T. Hotta and E. Dagotto, Phys. Rev. Lett. **88**, 017201 (2002).

[9] S. L. Cooper, Structure and Bonding **98**, 164 (2001), and references therein.

[10] M. W. Kim, J. H. Jung, K. H. Kim, H. J. Lee, J. Yu, T. W. Noh, and Y. Moritomo, Phys. Rev. Lett. **89**, 016403 (2002).

[11] S. Nakatsuji and Y. Maeno, J. Solid State Chem. **156**, 26 (2001).

[12] H. J. Lee, J. H. Jung, Y. S. Lee, J. S. Ahn, T. W. Noh, K. H. Kim, and S.-W. Cheong, Phys. Rev. B **60**, 5251 (1999).

[13] J. S. Lee, Y. S. Lee, T. W. Noh, K. Char, Jonghyurk Park, S.-J. Oh, J.-H. Park, C. B. Eom, T. Takeda, and R. Kanno, Phys. Rev. B **64**, 245107 (2001).

[14] A. V. Puchkov, M. C. Schabel, D. N. Basov, T. Startseva, G. Cao, T. Timusk, and Z.-X. Shen, Phys. Rev. Lett. **81**, 2747 (1998).

[15] T. Katsufuji, M. Kasai, and Y. Tokura, Phys. Rev. Lett. **76**, 126 (1995).

[16] M. Imada, A. Fujimori, and Y. Tokura, Rev. Mod. Phys. **70**, 1039 (1998), and references therein.

[17] For metallic samples, $\sigma(\omega)$ between 4.2 K and 300 K were obtained, but showed little T-dependence. And, the Ca_2RuO_4 sample was too small for us to take its T-dependent spectra.

[18] C. S. Alexander, G. Cao, V. Dobrosavljevic, S. McCall, J. E. Crow, E. Lochner, and R. P. Guertin, Phys. Rev. B **60**, R8422 (1999).

[19] S. Sugano, Y. Tanabe, and H. Kamimura, *Multiplets of Transition-Metal ions in Crystals* (Academic Press, New York and London, 1970).

[20] The energy costs given in Fig. 3 were evaluated in the atomic picture. If the full multiplicity is taken into account, the d^3 final state in the FM/AFO configuration corresponds to the term $^4A_2$, an eigenstate of the t_{2g}^3 configuration. [See Ref. [19].] Then, the excitation energy for the FM/AFO configuration should be $U - 4J$.

[21] S. Nakatsuji and Y. Maeno, Phys. Rev. B **62**, 6458 (2000).

[22] D. Singh, J. Appl. Phys. **79**, 4818 (1996); K. Fujioka, J. Okamoto, T. Mizokawa, A. Fujimori, I. Hase, M. Abbate, H. J. Lin, C. T. Chen, Y. Takeda, and M. Takano, Phys. Rev. B **56**, 6380 (1997).

[23] The fittings with Gaussian functions also give similar behaviors of S_α and S_β, although their absolute values are different by about 50 %.

[24] J. H. Jung, H. J. Lee, T. W. Noh, and Y. Moritomo, J. Phys.: Condens. Matter **12**, 9799 (2000).

[25] S. Sakita, S. Nimori, Z. Q. Mao, Y. Maeno, N. Ogita, M. Udagawa, Phys. Rev. B **63**, 2001 (2001).

FIGURES

FIG. 1. Doping-dependent $\sigma(\omega)$ of $Ca_{2-x}Sr_xRuO_4$ at room temperature. $\sigma(\omega)$ of x=0.0 is shown in the lower panel shifted downward by 500 $\Omega^{-1}cm^{-1}$. The inset shows $\Delta\sigma(\omega) = \sigma(\omega) - \sigma(\omega)_{x=2.0}$.

FIG. 2. (a) T-dependent $\sigma(\omega)$ of x=0.06. The contribution of the p-d transitions is indicated as a dot-dot-dashed line. The inset shows T-dependent ρ_{dc}. (b) The subtracted $\sigma(\omega)$ of the insulating state. Contributions of the p-d transitions and phonons were subtracted from each spectrum. The inset shows softening of a phonon peak with decreasing T.

FIG. 3. The spin/orbital configurations of t_{2g} orbitals at the two lattice sites: (a) FM/FO, (b) FM/AFO, (c) AFM/FO, and (d) AFM/AFO. Possible optical excitations are also shown in each configuration. (e) Jahn-Teller-like structural distortion induced by the doubly occupied d_{xy} and d_{zx} orbital with the AFO configuration. Octahedron at the left and the right side are flattened to the z and the x axis, respectively. (f) A schematic energy level in the AFM/AFO configuration with the Jahn-Teller-like distortion. The $U - J + 3E_{ph}$ excitation appears instead of the $U - J$ excitation.

FIG. 4. T-dependent spectral weights and ω_{TO}. $S_\alpha(T)$ are subtracted by the value at 100 K to give $\Delta S_\alpha(T)$ ($= S_\alpha(T) - S_\alpha(T$=100K)), and $S_\beta(T)$ are subtracted by the value at 220 K to give $\Delta S_\beta(T)$ ($= S_\beta(T) - S_\beta(T$=220 K)).
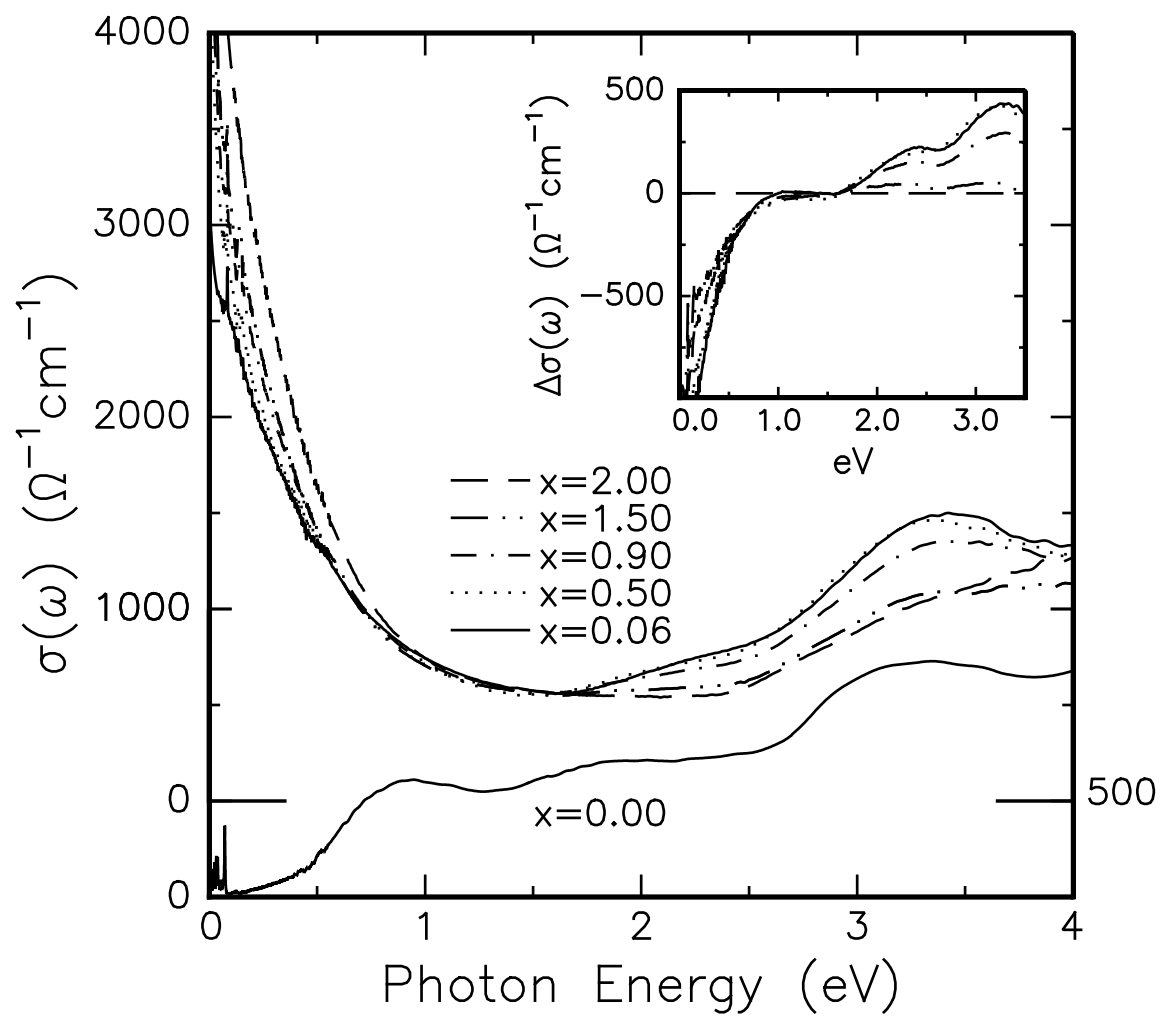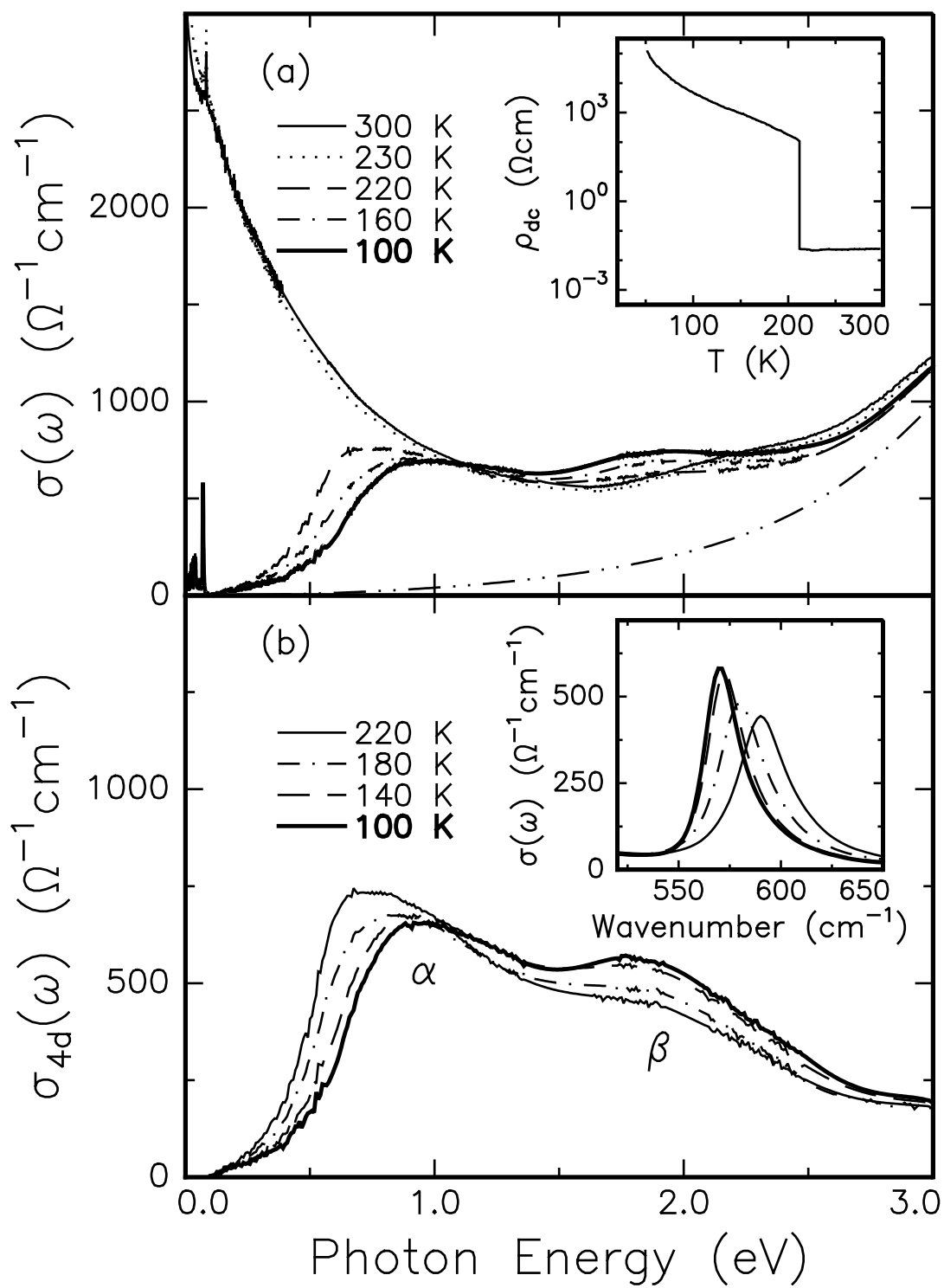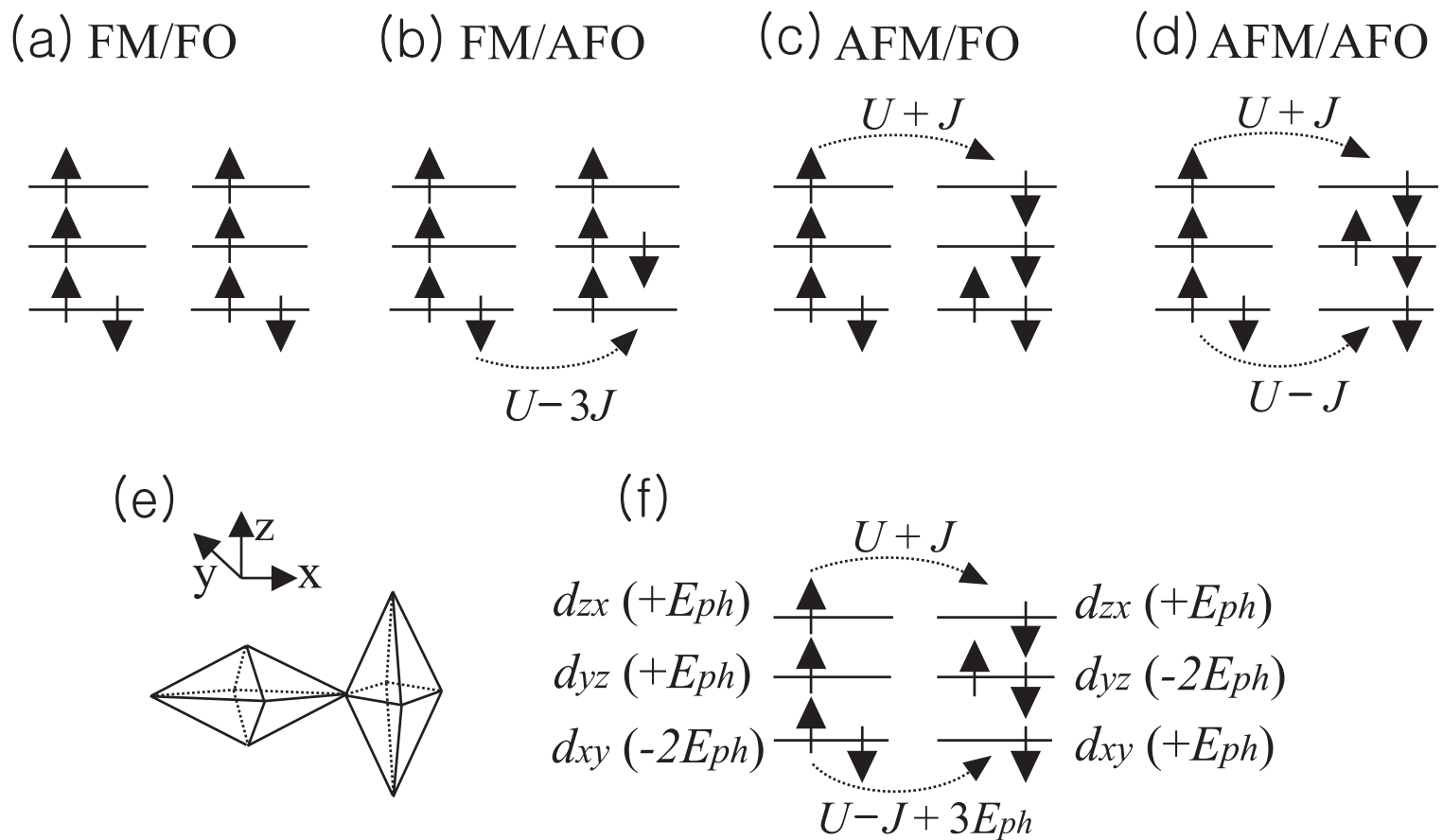
Fig. 1 J. S. Lee et al.

Fig. 2 J. S. Lee et al.

(a) FM/FO

(b) FM/AFO

$U-3J$

(c) AFM/FO

$U+J$

(d) AFM/AFO

$U+J$

$U-J$

(e)

z

y

x

(f)

$U+J$

d_{zx} (+E_{ph}) d_{zx} (+E_{ph})

d_{yz} (+E_{ph}) d_{yz} (-2E_{ph})

d_{xy} (-2E_{ph}) d_{xy} (+E_{ph})

$U-J+3E_{ph}$

Fig. 3 J. S. Lee et al.

ΔS_{β}

ω_{TO}

ΔS_{α}

Fig. 4 J. S. Lee et al.